# Electric-field-induced layer buckling in chiral smectic-*A* liquid crystals

R. E. Geer,[1,*] S. J. Singer,[2] J. V. Selinger,[1] B. R. Ratna,[1] and R. Shashidhar[1]
[1]*Center for Bio/Molecular Science and Engineering, Naval Research Laboratory, Code 6900, 4555 Overlook Avenue, SW, Washington, D.C. 20375*
[2]*Department of Chemistry, Ohio State University, Columbus, Ohio 43210*
(Received 28 October 1997)

X-ray-scattering data from chiral smectic-*A* liquid crystals under an applied electric field have been analyzed to investigate the layer-buckling instability. A quantitative description of the scattering data at all values of the field is obtained via calculation of the minimal-energy layer displacement profiles determined from the continuum smectic free energy. From this analysis the real-space layer-buckling profiles are determined, revealing a sinusoid to soliton evolution with increasing field. [S1063-651X(98)12303-6]

PACS number(s): 61.30.Eb, 61.30.Jf

Layered systems subjected to dilative strain along the modulation axis can develop a second modulation perpendicular to the original layer normal. This ''buckling'' brings the local layer spacing closer to its equilibrium value in the absence of any mechanism for injecting new layers. Layer buckling has been observed in many systems. It can be induced by temperature variation or magnetic fields in magnetic garnet films [1], by a dilative strain in homeotropically aligned smectic-*A* (Sm*A*) liquid crystals [2], and by temperature-induced molecular tilting in planar-aligned smectic-*C** (Sm*C**) liquid crystals [3]. More recently, substantial efforts have focused on chiral Sm*A** systems in which an electric field in the plane of the smectic layers induces a molecular tilt (the electroclinic effect [4]), thus reducing the equilibrium layer spacing and producing a dilative strain. This strain leads to a buckling of the layers and an in-plane modulation of the director, which affects the optical properties of the material [5]. Since these materials have real potential in fast-switching, gray-scale optical devices, the formation of an in-plane modulation is of significant scientific and practical interest [6–8].

In this paper we present the results of synchrotron x-ray scattering measurements on a Sm*A** liquid crystal exhibiting a large electroclinic effect and a pronounced electric-field-induced layer buckling. Analysis of the x-ray data reveals an evolution from a sinusoidal layer profile to a zigzag or soliton profile as the field is increased. We quantitatively describe this evolution on the basis of a continuum elastic theory for a smectic liquid crystal under dilative strain. Excellent agreement is obtained between theory and experiment for all values of the field.

The liquid-crystalline material under investigation, KN125 [7,9], consists of chiral, thermotropic mesogens with a negative dielectric anisotropy. It is confined between two indium tin oxide (ITO) coated glass plates with rubbed polyimide surface layers (EHC Ltd. Japan) that induce planar alignment of the smectic director [schematically depicted in Fig. 1(a)]. The cell thickness is 2 $\mu$m and the ITO electrodes extend over a 16-mm$^2$ area. Initial alignment of the smectic director is obtained by slowly cooling the sample through the isotropic-Sm*A* phase transition (78 °C) in the presence of a small (1 V/$\mu$m) ac electric field. All x-ray-scattering measurements were performed at $45\pm0.05$ °C at beam line X-23B at the National Synchrotron Light Source. The measurements were taken as a function of electric field with a 10-Hz square wave. (An ac field was used in order to avoid degra-

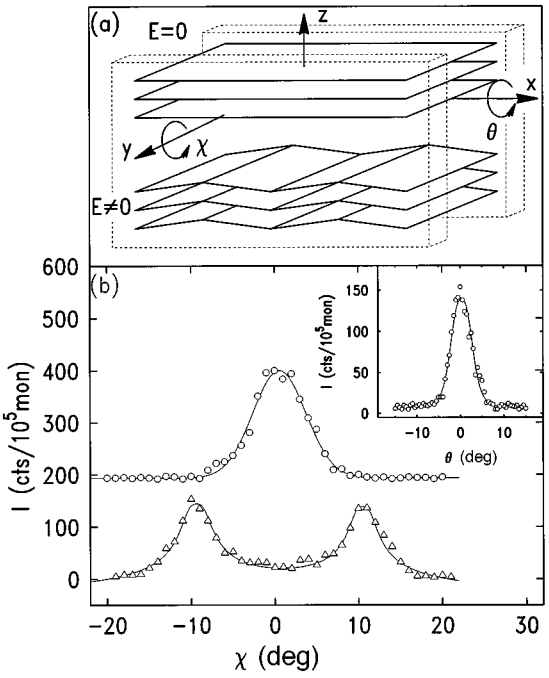


FIG. 1. (a) Schematic of layer buckling in a liquid-crystal cell (dotted lines refer to glass cell walls). X-ray $\chi$ and $\theta$ scans rotate the cell about the $y$ and $x$ axes, respectively. As an electric field $E$ is applied, the equilibrium layer spacing is reduced, resulting in a distortion of the layers along the $x$ axis. For high fields, the distortion has the zigzag or soliton form shown. (b) $\chi$ scans across the Bragg reflection at $E=1$ V/$\mu$m (open circles) and $E=14$ V/$\mu$m (open triangles). The peak splitting at high fields indicates the presence of a soliton distortion. Inset: $\theta$ scan across the Bragg reflection at $E=1$ V/$\mu$m. No splitting is evident at this or any field, confirming that the smectic director lies in the $xz$ plane. This peak narrows slightly at higher fields. The units of scattering intensity are scattered photons per $10^5$ incident (or monitor) counts.

*Present address: Department of Physics, State University of New York at Albany, Albany, NY 12222.

 

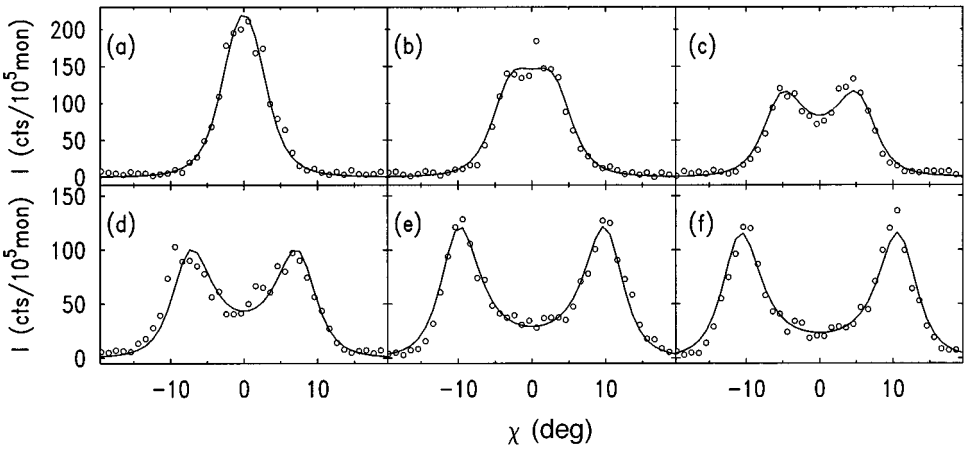


FIG. 2. (a)–(f) $\chi$ dependence of scattered x rays (open circles) at the Bragg reflection at $E=1$, 2, 4, 7, 10, and 14 V/$\mu$m, respectively. The evolution of the peak separation is clearly evident. Solid lines represent best fits to the model described in the text. Agreement is very good for all values of $E$.

dation of the sample; the results are independent of frequency for frequencies much less than the inverse response time of the liquid crystal.) The scattering geometry has been described in detail elsewhere [7]. X-ray scan directions are summarized in Fig. 1(a). The $z$ axis defines the polyimide rubbing direction and the average layer normal. When the x-ray-scattering angle is fixed at the Bragg reflection of the layers, $\theta$ scans rotate the sample about the $x$ axis and probe angular variations of the layer normal along the $y$ axis. Likewise, $\chi$ scans rotate the sample about the $y$ axis and probe layer-normal variations along the $x$ axis.

In these cells, field-induced molecular tilting leads to layer buckling, which is manifest as an angular splitting in the Bragg reflection along a $\chi$ scan. At the lowest fields (minimal or zero buckling) a single peak is centered at $\chi=0°$. At higher fields the layer planes become sharply kinked [Fig. 1(a)], with two distinct normals at an angular offset to the $z$ axis. The latter case is the soliton limit [7,8]. The $\chi$ dependence of the scattered x-ray intensity corresponding to these limits is shown in Fig. 1(b). The existence of a soliton layer distortion is implied in the high-field ($E=14$ V/$\mu$m) data by the intensity at $\chi=0°$, which is near background, i.e., a very small fraction of the smectic director parallel to the $z$ axis. The angular offset of the buckled-layer planes from the $z$ axis at this field is approximately 10°. $\theta$ scans reveal the angular distribution of the layer normal in the $y$ direction. A sharp peak at $\theta=0°$ in the inset of Fig. 1(b) implies confinement of the smectic director in the $xz$ plane, which persists at all values of $E$. Polarized optical microscopy and optical diffraction show that the buckling period in the $x$ direction is $\Lambda=4$ $\mu$m, independent of $E$.

The evolution of the $\chi$ scattering was measured for $E=1$, 2, 3, 4, 5.5, 7, 8.5, 10, 12, and 14 V/$\mu$m. The results are shown in Fig. 2 for selected values of $E$. A continuous separation of the peaks is evident, along with a decrease in the scattering at $\chi=0°$. Except at the highest fields, the scattered intensity at $\chi=0°$ exceeds that expected from a simple overlap of the two separate $\chi$ peaks. This argues against a simple soliton picture at low fields. Quantitatively, these results represent a convolution of the instrumental resolution with the distribution function of the smectic director in the $xz$ plane,

$$I(\chi)=\int_{-\infty}^{\infty}d\omega'\int_{-\Lambda/2}^{\Lambda/2}dx\ \delta(\omega'-\omega(x))R(\chi-\omega')$$
$$=\int_{-\Lambda/2}^{\Lambda/2}dx\ R(\chi-\omega(x)). \tag{1}$$

Here $\omega(x)$ is the angle between the local layer normal and the $z$ axis. The resolution function $R(\chi-\omega)$ includes both the instrumental resolution and the smectic director mosaicity arising from defects occurring during cell filling and initial sample alignment [10]. This mosaicity is significantly larger than the instrumental resolution and is slightly sample and field dependent.

These experimental results can be compared with theoretical predictions for the layer profile. The continuum free energy for layer distortions is

$$F=\int d\mathbf{r}\left(\frac{B}{2}\left\{\frac{\partial U}{\partial z}-\frac{1}{2}\left[\left(\frac{\partial U}{\partial x}\right)^2+\left(\frac{\partial U}{\partial y}\right)^2\right]\right\}^2+\frac{K}{2}\left(\frac{\partial^2 U}{\partial x^2}+\frac{\partial^2 U}{\partial y^2}\right)^2\right), \tag{2}$$

where $U(\mathbf{r})$ is the displacement of layers from their equilibrium position at $E=0$. Under a field, the molecules tilt by an angle of $\Theta(E)$ and the equilibrium layer spacing contracts to $d(E)=d_0\cos\Theta(E)$. The system therefore experiences a dilative strain of $\alpha=1-d(E)/d_0$. The displacement can then be written as $U(\mathbf{r})=\alpha z+u(x,y)$, where $u(x,y)$ accounts for deviations from uniform strain. Since layer modulation is observed only along the $x$ direction, we minimize $F$ over displacement functions of a single variable $u(x)$. This minimization leads to the Euler-Lagrange equation

$$\lambda^2\frac{\partial^2\omega}{\partial x^2}=-\frac{\partial}{\partial\omega}\left[\frac{\alpha}{2}\omega^2-\frac{1}{8}\omega^4\right], \tag{3}$$

where $\omega(x)\equiv\partial u/\partial x$. This equation is isomorphic to the classical equation of motion for a particle in an inverted quartic potential.

One solution to this equation was found by Pavel and Glogarova [11]. They performed the minimization for an infinite sample with a single deformation (kink) and found the soliton solution

$$\omega(x)=\sqrt{2\alpha}\,\tanh\left(\frac{\sqrt{2\alpha}}{2\lambda}\,x\right), \tag{4}$$

where $\lambda=\sqrt{K/B}$. This equation shows that the width of a kink, the region over which the layers bend, is $\lambda/\sqrt{\alpha}$. They then constructed a periodic profile by adding subsequent kinks at successive half periods. This periodic profile is only valid when the kink width $\lambda/\sqrt{\alpha}$ is much smaller than the period $\Lambda$. We attempted to fit this periodic profile to the scattering data in Fig. 2 with three fitting parameters: the length $\lambda$, the strain $\alpha$, and the mosaicity $\xi$. It was impossible to fit the data without using unphysically large values of $\lambda$ ($\sim 1\ \mu$m) [12] or values of $\alpha$ that disagreed with previous measurements of the tilt angle [7,9]. Specifically, the Pavel-Glogarova model was unable to account for the scattering near $\chi=0°$ for $E<12$ V/$\mu$m, where the kink width is not much less than the period. These results showed the need for a general minimization of the free energy in the presence of strain that is valid when the layer curvature is not localized in defect or soliton walls.

A general minimization of the free energy was performed by Singer in another context [13]. His calculation shows that the Euler-Lagrange equation has a family of periodic solutions given by

$$\omega(x)=\sqrt{2\alpha\zeta_-}\,\mathrm{sn}\left(\frac{\sqrt{2\alpha\zeta_+}}{2\lambda}\,x\middle|\frac{\zeta_-}{\zeta_+}\right), \tag{5}$$

where $\mathrm{sn}(u|m)$ is a Jacobi elliptic function and $\zeta_\pm=1\pm\sqrt{1-\varepsilon}$. The solutions are indexed by the parameter $\varepsilon$, the particle energy in the classical analogy scaled so that $0<\varepsilon<1$. In the limit $\varepsilon\to 0$, the buckling pattern is sinusoidal. In the opposite limit $\varepsilon\to 1$, the solution reduces to Eq. (4) and the pattern has a zigzag or soliton character. The buckling wavelength $\Lambda$, corresponding to the period of motion in the mechanical analogy, is related to $\alpha$ and $\varepsilon$ by

$$\Lambda=\lambda\sqrt{\frac{32}{\alpha\zeta_+}}\,K\left(\frac{\zeta_-}{\zeta_+}\right), \tag{6}$$

where $K(m)$ is the complete elliptic integral of the first kind.

Equation (5) gives the angular profile $\omega(x)$ of the layer orientation. The corresponding layer displacement profile $u(x)$ is the integral of $\omega(x)$. These results are expressed in terms of the two parameters $\alpha$ and $\varepsilon$. The strain $\alpha=1-d(E)/d_0$ is determined by the field $E$; as an approximation we assume $\alpha=CE$ [14]. The parameter $\varepsilon$ is determined implicitly by Eq. (6) in terms of the wavelength $\Lambda$ and the length $\lambda$. As noted above, optical experiments show that the wavelength is $\Lambda=4\ \mu$m, independent of $E$. Thus, for each value of $E$, the theory predicts $\omega(x)$ and $u(x)$ in terms of the two parameters $C$ and $\lambda$. The angular profile $\omega(x)$, together with the mosaic function $R(\chi-\omega)$, determines the x-ray-scattering intensity $I(\chi)$ for comparison with experiment. Our approach was to perform a nonlinear least-squares fit to the data for *all ten* values of $E$ simultaneously, with three *field-independent* fitting parameters: the length $\lambda$, the coefficient $C$, and the mosaicity $\xi$ [15].

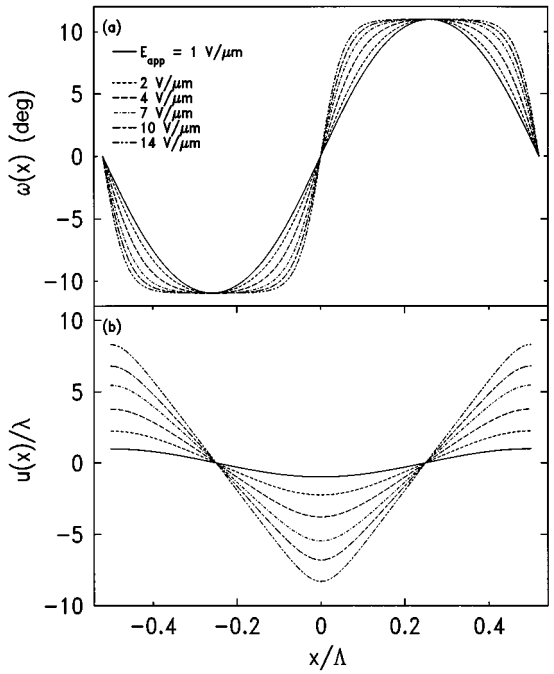


FIG. 3. (a) Angular profile of smectic director orientation as a function of $E$, as determined from analysis of the data in Fig. 2. The narrowing of the defect or kink region with increasing $E$ is clearly evident. (b) Corresponding layer-buckling profile. An evolution from a low-amplitude sinusoid at low fields to a high-amplitude soliton profile at high fields can be seen.

The fitting results are shown in Fig. 2. Agreement with experiment is excellent, keeping in mind that only three field-independent parameters are used to fit the entire data set. The first parameter is $\lambda=\sqrt{K/B}=199$ Å, which is relatively high for Sm*A* materials. However, the elastic constants $K$ and $B$ are not known for KN125 and this large $K/B$ ratio may be responsible for the large electroclinic effect in this material. The second parameter is $C=1.33\times 10^{-3}$ $(\mathrm{V}/\mu\mathrm{m})^{-1}$, which agrees with the value $C=1.5\times 10^{-3}$ $(\mathrm{V}/\mu\mathrm{m})^{-1}$ determined from the Bragg wave vector as a function of $E$. It is also consistent with optical measurements of the tilt angle [7,9]. The third parameter is $\xi=4.28°$, which includes the spectrometer resolution (approximately 0.35°) and agrees with the range of mosaicities (3.7°–4.4°) observed in similar samples. The angular profiles $\omega(x)$ and layer displacement profiles $u(x)$ derived from these fits are shown in Fig. 3. The evolution from a sinusoid at the lowest field to a soliton profile at higher fields is evident. Note also the increase in the amplitude of the modulation with increasing field.

We point out that this system has a threshold strain for the onset of buckling, which arises because the wavelength $\Lambda$ is independent of $E$. Equation (6) implies that a decrease in the strain $\alpha$ leads to a decrease in $\varepsilon$. At the threshold strain $\alpha_{\mathrm{threshold}}=(2\pi\lambda/\Lambda)^2$, $\varepsilon\to 0$. For $\alpha<\alpha_{\mathrm{threshold}}$ there is no periodic solution to the Euler-Lagrange equation with the fixed wavelength $\Lambda$. Using the values of $\lambda$ and $C$ determined from the fit, the threshold strain is $9.9\times 10^{-4}$, which implies a threshold field of 0.66 V/$\mu$m. This value is less than the

minimum field of 1 V/$\mu$m necessary for smectic director alignment and is consistent with the appearance of weak buckling during that procedure. Unfortunately, smaller alignment fields are not sufficient to remove focal conic defects, which is necessary for reliable x-ray-scattering data. Since relaxation of weak layer buckling is very slow in these samples, data were only analyzed for $E \geqslant 1$ V/$\mu$m.

Finally, we note that our theory does not address the issue of wavelength selection in layer buckling. Instead, our theory assumes that the layers buckle with a fixed wavelength $\Lambda$ and derives the resulting buckling profile. In most systems that exhibit layer buckling, the buckling wavelength depends on the strain [1–3]. However, in this system, optical experiments show that the wavelength is independent of $E$ and is approximately twice the cell thickness. This wavelength has not been explained by any theory based on an equilibrium free energy. The wavelength may be determined by nonequilibrium considerations, such as the past history of the distortion [16] or flow patterns [17]. Once the system selects an initial buckling wavelength through any mechanism, it may be difficult for the system to change its wavelength in response to changes in $E$. Any change in wavelength requires a large-scale rearrangement of the layers, which might not come to equilibrium in the experimental time scale. In contrast, a change in the shape of the layers requires only a local rearrangement of the molecules, which should reach equilibrium much more quickly. Thus it is reasonable that our equilibrium theory can predict the buckling profile, even if it cannot predict the wavelength.

In conclusion, an investigation of field-induced layer buckling in chiral Sm*A* liquid crystals has been presented. An analysis of scattered synchrotron x-ray radiation by minimization of the free energy in the presence of strain reveals an evolution from a sinusoid to a soliton layer buckling. A description of this evolution requires a full, periodic solution of the Euler-Lagrange equation.

We thank J. Naciri for the liquid-crystal sample and N. A. Clark and D. M. Walba for helpful discussions. This research was supported by the Office of Naval Research.

[1] M. Seul and R. Wolfe, Phys. Rev. Lett. **68**, 2460 (1992); Phys. Rev. A **46**, 7519 (1992).
[2] N. A. Clark and R. B. Meyer, Appl. Phys. Lett. **22**, 493 (1973).
[3] T. P. Rieker and N. A. Clark, in *Phase Transitions in Liquid Crystals*, edited by S. Martelucci (Plenum, New York, 1992).
[4] S. Garoff and R. B. Meyer, Phys. Rev. Lett. **38**, 848 (1977).
[5] J. R. Lindle *et al.*, Proc. SPIE Int. Soc. Opt. Eng. **2408**, 40 (1995); Appl. Phys. Lett. **70**, 1536 (1997).
[6] M. Johno *et al.*, Ferroelectrics **114**, 611 (1991).
[7] G. P. Crawford *et al.*, Appl. Phys. Lett. **65**, 2937 (1994).
[8] A. G. Rappaport *et al.*, Appl. Phys. Lett. **67**, 362 (1995).
[9] G. P. Crawford, J. Naciri, R. Shashidhar, and B. R. Ratna, Jpn. J. Appl. Phys., Part 1 **35**, 2176 (1996).
[10] For the spectrometer used for this work the function is $R(\chi-\omega) \propto [1+\xi^2(\chi-\omega)^2]^{-2}$.
[11] J. Pavel and M. Glogarova, Liq. Cryst. **9**, 87 (1991).
[12] P. G. de Gennes, *The Physics of Liquid Crystals* (Oxford, New York, 1975).
[13] S. J. Singer, Phys. Rev. E **48**, 2796 (1993).
[14] In principle, the strain $\alpha$ can be obtained directly from the data for the Bragg wave vector $q$ as a function of electric field $E$. However, our $q$ vs $E$ data are fairly noisy, so they do not give good-quality fits for the line shapes. For that reason, we assume the relation $\alpha = CE$ and determine $C$ in two ways: from a fit of the line shapes and from a fit of the $q$ vs $E$ data. These two approaches give approximately the same value of $C$.
[15] The mosaicity $\xi$ has a slight field dependence; it varies by approximately 15% over the range of fields investigated. For simplicity, we used a single mosaicity to describe the entire data set and allowed it to vary over this 15% range. This variation affected the quality of the fit, but had no effect on the values of the other parameters.
[16] R. F. Shao, P. C. Willis, and N. A. Clark, Ferroelectrics **121**, 127 (1991).
[17] A. B. Davey and W. A. Crossland, Mol. Cryst. Liq. Cryst. **263**, 325 (1995).